Isoconversional thermal decomposition reaction kinetics of oil palm trunk and rubberwood sawdust for thermochemical conversion processes

Pranshu Shrivastava[1] · Arkom Palamanit[2] · Anil Kumar[3,4]

Abstract

Biomass as a raw material has profound implications for thermal conversion processes. It is important to study the relationship between kinetic modeling to depict significant importance in thermal processing by estimating volatile yield and reaction performance during biomass decomposition. This work aimed to determine the thermal decomposition reaction kinetics of non-woody (oil palm trunk (OPT)) and woody (rubberwood sawdust (RWS)) biomass. Devolatilization of biomass is determined by the thermogravimetric analysis (TGA) at three different heating rates (10, 20, and 30 °C/min) using nitrogen as inert gas. The kinetic analysis used isoconversion models of Friedman, Ozawa-Flynn-Wall (OFW), and Kissinger–Akahira–Sunose (KAS). The activation energy varied from 218.4 to 303.8 kJ/mol (Friedman), 235.9 to 299.1 kJ/mol (OFW), and 235.8 to 298.9 kJ/mol (KAS) for OPT; and 199.7 to 228.1 kJ/mol (Friedman), 210.6 to 225.6 kJ/mol (OFW), and 210.7 to 225.2 kJ/mol (KAS) for RWS. The kinetic analysis indicated that RWS and OPT had diverse reaction kinetics, which depend on the reaction rate and order of the reaction. Experimental and theoretical conversion data agreed reasonably well, indicating that these results can be used for future OPT and RWS process modeling. Consistency of results is validated using GC–MS equipped with a pyrolyzer.

Keywords Biomass · Kinetic analysis · Thermal analysis · Oil palm · Rubberwood · Pyrolysis

Introduction

Concerns about environmental safety and sustainability have prompted the development of novel processing technologies for converting renewable energy sources such as biomass agro-residues to energy, chemicals, and bioproducts. Between 2019 and 2020, Thailand's palm oil sector recorded a world output of 41.9 million tonnes (Shahbandeh 2020). The immense worldwide interest in palm oil (with around 27% offer of the aggregate world's oil and fat creation) has caused an expansion in oil palm generation, which has also encouraged the age of vast measure of oil palm waste (OPW). In 2020, Thailand had a cultivated area of rubber and oil palm tree, 34.08 and 0.92 million ha, respectively, and most of them were grown in southern Thailand, i.e., 71.3% and 86.8%, respectively. Furthermore, old rubber trees and rubber wood processing contribute to the increased production of biomasses such as roots, bark, sawdust, and branches. Also, old oil palm trees and processing of fresh

Responsible Editor: Guilherme Luiz Dotto

✉ Anil Kumar
anilkumar76@dtu.ac.in

1 Department of Mechanical and Mechatronics Engineering, Faculty of Engineering, Prince of Songkla University, Hat Yai, Songkhla 90110, Thailand

2 Biomass Energy and Sustainable Technologies (BEST) Research Center, Energy Technology Program, Department of Interdisciplinary Engineering, Faculty of Engineering, Prince of Songkla University, Hat Yai, 90110 Songkhla, Thailand

3 Department of Mechanical Engineering, Delhi Technological University, Shahbad Daulatpur, Delhi 110042, India

4 Centre for Energy and Environment, Delhi Technological University, Shahbad Daulatpur, Delhi 110042, India

fruits in crude palm oil production generate kernel, fiber, empty fruit shell, fronds, and trunk (Yusoff 2006; Shuit et al. 2009; Sulaiman et al. 2011; Loh 2017). Some rubberwood and oil palm have been utilized as fuels for traditional heat and power combustion methods. Traditionally, the energy produced from crude oil or coal by direct combustion is adequate rather than biomass. Scarcity in fossil reserves encourages the usage of biomass as a feedstock to produce energy. Pyrolysis is the most common conversion process that converts biomass into biochar and bio-oil (Palamanit et al. 2019). Biochar and bio-oil can be treated as an alternative to coal and oil from pyrolysis. Pyrolysis is considered old technology, but it has been improved recently and is also becoming more captivating than other conversion processes (Mohan et al. 2006; Hu and Gholizadeh 2019).

Generally, the pyrolysis process comprises a very complex set of reactions involving forming radicals, resulting in bio-oil, and biochar forming (Yaman 2004). Pyrolysis process is conducted in an oxygen deficient environment. This process occurs in three stages; in the first stage, up to 150 °C of light volatile matter and moisture evaporates. In the second stage, a constant heat source broke down higher molecular weight molecules into lower molecular weight chemicals (150–600 °C). Most of the volatiles that included condensable and non-condensable gases were mainly decomposed and released by cellulose and hemicellulose, hence known as active pyrolytic stage. Finally, lignin thermally transformed at a slower pace at high temperatures (> 600 °C) in the third stage, assisted by hydroxyl phenolic compounds that enhanced biomass thermal stability. Oil palm empty fruit bunches, palm kernel shells, hazelnut husk, *Samanea saman* seeds, and distinct types of sawdust were studied using TGA analyzer. These studies reported that biomasses decomposed majorly through three stages (Ceylan and Topçu 2014; Mishra and Mohanty 2019; Mishra et al. 2019, 2020; Rueda-Ordóñez et al. 2019). In addition, lignin presence in sample at a higher proportion contributed to char formation, which can be used in various applications (Mishra and Mohanty 2019; Rueda-Ordóñez et al. 2019; Pielsticker et al. 2021).

An important parameter that needs to discuss before the conversion of biomass is the kinetic analysis. Process parameters such as optimization, design of pyrolysis, and gasification reactors can be decided on the information provided by the kinetic analysis of biomass. Furthermore, it discusses mathematical modeling simplification and kinetic analysis parameters such as activation energy (E_a) and frequency factor (A). The simplest analytical tool to analyze reaction and its kinetic behavior for various thermochemical conversion processes is the thermogravimetric (TGA) analysis. It is considered one of the most widely used techniques for studying devolatilization process of biomass pyrolysis. This process is known to observe the decomposition of biomass in terms of

mass concerning either time or temperature in a controlled manner (Huang et al. 2016; Ojha et al. 2021a). There are two methods for conducting TGA studies: isothermal and non-isothermal. The isothermal model is less frequently used than the non-isothermal model because it is less accurate. In an isothermal experiment, very little weight loss is seen before the appropriate temperature is reached, which causes the kinetic parameters to be estimated incorrectly. Kinetic parameters can be determined more quickly and effectively using non-isothermal approaches. The examination of TGA data can be done using a variety of techniques. Model fitting approach and model-free (isoconversion) methods are popularized to provide pertinent information about the process.

The model fitting approach consists of a different type of model than fitting data for achieving an acceptable and fitting statistical best. The model-free approach offers kinetic parameters such as activation energy and pre-exponential factor with no assumptions using various heating rate curves (Slopiecka et al. 2012; Pielsticker et al. 2021). Isoconversional (multi-heating) methods can estimate complex material reactions. These approaches are straightforward, and best benefit is that there is no chance of choosing the wrong kinetic model and finding wrong kinetic parameters (Alwani et al. 2014; Pattanayak et al. 2021). The Friedman, Ozawa-Flynn-Wall (OFW), and Kissinger–Akahira–Sunose (KAS) methods are based on an isoconversion model. Generally, model-free models generate very few errors (less than 1%) (Mishra and Mohanty 2020). These methods only apply to an independent model's kinetic parameter estimation of a narrow conversion range (mostly 0.1–0.7).

Over the past several decades, several researchers have investigated pyrolysis activities of different biomasses and their kinetics (Xiao et al. 2020; Mishra et al. 2023). Hemicellulose devolatilization and lignin are the first, and cellulose devolatilization is the second. Researchers have also studied the effect of heating rates on pyrolysis of different biomasses and discussed the effect of heating rates on pyrolysis kinetics in terms of activation energy (Ojha et al. 2021b; Tian et al. 2021; Peterson et al. 2022). Li et al. (2021) performed non-isothermal forest waste pyrolysis at varying heating rates and showed that to obtain kinetic parameters, an optimization method is in good agreement with experimental findings. While numerous notable biomass kinetics studies have been published, no such studies are available to determine pyrolysis reaction kinetics of the oil palm trunk and rubberwood sawdust waste. Therefore, this research focused on physiochemical characteristics of these waste biomasses and their thermal degradation behavior (kinetic analysis). In the present research, three different heating rates were selected to understand the kinetic degradation phenomenon of OPT and RWS. The rates are 10 °C/min, 20 °C/min, and 30 °C/min. In addition, 10 °C/min increment in heating rate

was chosen to understand the most precise phenomenon. Due to shifting peaks during TGA pyrolysis, long periods are insufficient for accurate results. Three model-free methods, including Friedman, Ozawa-Flynn-Wall (OFW), and Kissinger–Akahira–Sunose (KAS) methods, are capable of measuring activation energy (E_a), which gives precise results since they are based on these models without making any assumptions.

Material and method

Physicochemical properties of biomass used

Oil palm trunk (OPT) and rubber wood sawdust (RWS) were agricultural residues examined in this work. First, their physical–chemical characteristics were determined (moisture, proximate analysis, ultimate analysis, and higher heating value). These characteristics are key parameters in determining biomass quality as a biofuel; therefore, this step is important for choosing the most effective thermochemical method. OPT was obtained from Krabi (Thailand), while RWS was obtained from a rubber wood processing plant in Songkla (Thailand). Fresh OPT was processed using a chopping machine (MCH-420, Machinery789, Thailand). The OPT and RWS were dried for 1 week using a solar greenhouse to reduce the moisture content necessary for pyrolysis. The dried samples were ground using a grinding machine with 1 mm filter (model YPS-102, Bonny, 2 hp, Thailand) and then placed in sealed plastic bags for further use.

Standard ASTM E871-82 has applied 10 g samples in an oven at 103.5 °C for 24 h to determine moisture content. The proximate analysis was determined according to standard ASTM D7582 using a macro thermogravimetric analyzer (TGA 701, LECO, USA). In contrast, ultimate analysis was determined according to EN 15104 and ASTM D4239 standards using a CHNS/O analyzer (FLASH 2000, Thermo Scientific, Italy). The oxygen content was determined based on the difference method. Finally, the higher heating value (HHV) and lower heating value (LHV) in MJ/kg were determined using Eqs. (1) and (2), in which H and M correspond to percentages of hydrogen and moisture in biomass, respectively (Monir et al. 2018).

$$\text{HHV(MJ/kg)} = 0.3491 * C + 1.1783 * H + 0.1005 * S \\ - 0.1034 * O - 0.0151 * N - 0.0211 * Ash \tag{1}$$

$$(\text{LHV})_{\text{dry}}(\text{MJ/kg}) = (\text{HHV})_{\text{dry}} - 2.442 * 88.936H/100 \tag{2}$$

Thermogravimetric analysis

Thermal analysis was conducted using a thermogravimetric analyzer (Perkin Elmer, USA). The samples' mass loss was measured from 50 to 1000 °C at heating rate that varies from 10, 20, and 30 °C/min under a nitrogen gas atmosphere. Tests have been conducted three times to achieve consistency and accuracy. The average value of volatized mass is calculated based on initial and final weights of the biomass after each experiment. Before each analysis, test samples were dried, and a vacuum pump was used to omit the trace oxygen from thermogravimetric analyzer.

Kinetic analysis and methods

Biomass is a complex blend of different materials, such as hemicellulose, cellulose, lignin, extractive, and small quantities of inorganic matter, in which each component has its spectrum of thermal decomposition. The study determined dehydration, volatile release and carbonization stages, and mass loss ranges corresponding to temperature. It is also very difficult to predict an exact kinetic reaction of pyrolysis. Thus, different models apply different approximation methods to calculate activation energies. A general mechanism of reaction for pyrolysis can therefore be written as follows:

$$\text{Biomass} \xrightarrow{k(t)} \text{Volatiles(gas + tar)} + \text{Char(solid residue)} \tag{3}$$
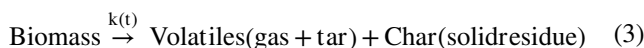
Rate of reaction for conversion of biomass from solid form to volatiles is written as follows:

$$\frac{dx}{dt} = k.f(x) \tag{4}$$

where x is rate of conversion at a particular time t. The rate of reaction is defined by Arrhenius equation as follows:

$$k = k_0 e^{-\left(\frac{E_a}{RT}\right)} \tag{5}$$

where E is activation energy expressed (kJ mol^{-1}), k represents reaction rate constant, k_o is pre-exponential factor (min^{-1}), T is absolute temperature (K), and R is gas constant (8.314 J mol^{-1} K^{-1}). The conversion of sample is function of temperature:

$$x = \left(\frac{m_0 - m_t}{m_0 - m_f}\right) \tag{6}$$

After solving Eqs. (4), (5), and (6):

$$\frac{dx}{dt} = k_o e^{-\left(\frac{E_a}{RT}\right)}(1 - x)^n \tag{7}$$

Heating rate is an important parameter during pyrolysis kinetics; it can be written as follows:

$$\beta = \frac{dT}{dt} = \frac{dT}{dx} \times \frac{dx}{dt} \tag{8}$$

After solving Eqs. (7) and (8):

$$g(x) = \int_0^x \frac{dx}{f(x)} = \int_0^T \frac{A}{\beta} e^{-(E/RT)} dT \tag{9}$$

$$g(x) = \frac{AE}{\beta R} \int_0^x u^{-2} e^{-u} du = \frac{AE}{\beta R} p(x) \tag{10}$$

where $g(x)$ is integral conversion and x is $\frac{E}{RT}$. However, $p(x)$ does not have an exact solution. Hence, numerical approximation can be obtained. $p(x)$ varies, referring to the approximation chosen for simplification.

Friedman method

The Friedman process used for kinetic analysis of samples is first and more general isoconversional method. This approach is based on differential techniques that minimize the likelihood of error. The equation for Friedman method is written as follows:

$$\ln\left(\frac{dx}{dt}\right) = -\frac{E}{RT} + \ln(A.f(x)^n) \tag{11}$$

Plot between $\ln\frac{dx}{dt}$ versus $1/T$ provides slope $-\frac{E}{RT}$ and intercept $\ln(A.f(x)^n)$

Ozawa–Flynn–Wall (OFW) method

Ozawa–Flynn–Wall (OFW) method uses Doyle's approximation, $p(x) = -2.315 + 0.457 \times$ to calculate the material's activation energy and frequency factor.

By substituting Doyle's approximation in Eq. (12):

$$\ln(\beta) = \ln\left[\frac{AE}{Rg(x)}\right] - 2.315 - 0.457\frac{E}{RT} \tag{12}$$

Plot between $\ln(\beta)$ and $1/T$ is used to calculate activation energy and pre-exponential factor.

Kissinger–Akahira–Sunose (KAS) method

This method is used to calculate kinetic energy by employing an isoconversional method. By applying an approximation of $p(x) = x^{-2} e^{-x}$ in Eq. (8); the linear plot of $\ln(\beta/T_{max}^2)$ versus $1000/T_{max}$, slope and intersection of a straight line can be used to determine the E_a, which can be calculated as follows (Huang et al. 2016):

$$\ln\left(\beta/RT_{max}^2\right) = -E_a/RT_{max} + \ln\left(A/E_a\right) \tag{13}$$

where T_{max} is maximum temperature, β is heating rate, A is pre-exponential or frequency factor, and R is the universal gas constant.

Gas chromatography using pyrolyzer

Py-GC–MS (Agilent 7890A, Germany) is used to analyze the pyrolytic behavior of oil palm trunk (OPT) and rubberwood sawdust (RWS) under nitrogen atmosphere. The column used in this study is Agilent HP-5MS (30 m × 250 μm × 0.25 μm). The initial conditions are 40 °C for the first 30 s, then increased at 10 °C/min to 600 °C while keeping 30 min total GC run time. Volatile fragments were investigated by comparing findings to those of earlier papers and fitting mass spectra from NIST spectral libraries. For quantitative calculations, percentage areas were calculated for each pyrolysis product component.

Results and discussion

OPT and RWS characterization

The initial characteristics of raw samples are listed in Table 1. Bioproduct yield during pyrolysis is highly influenced by biomass physicochemical properties (Pattiya and Suttibak 2012a; Palamanit et al. 2019; Shrivastava et al. 2020). All biomass samples were found with high volatile matter content, which also influenced the activation energies of biomass used in the study. RWS has highest VM and least ash contents than OPT, leading to a high liquid yield as discussed in previous studies (Mckendry 2002b; Chen et al. 2008). OPT had a greater FC relative to RWS. Carbon contents of RSW and OPT were relatively high compared to cassava rhizomes, cassava stalk, wheat straw, corn stalk, wood sawdust, corncob, rice husk, bamboo, oak wood, and birch wood (Pattiya and Suttibak 2012a, b; Biswas et al. 2017; Mishra and Mohanty 2018; Widjaya et al. 2018). Biomass with a high carbon and hydrogen content usually has a high HHV and LHV, as shown in Table 1 (Uzun et al. 2016; Palamanit et al. 2019).

Previous studies suggested that if the contents of nitrogen and sulfur in biomass samples are low then it helps prevent partial formation of nitrogen oxides and sulfur oxides during the biomass oxidation of nitrogen and sulfur (Mishra and Mohanty 2019; Palamanit et al. 2019). Bulk density (considered one of the important parameters while studying characteristics of biomass) was least in OPT followed and RWS, an essential parameter for designing reactor for pyrolysis system. The bulk density of biomass particles directly affects volume of biomass present in the reaction chamber

Table 1 Physicochemical properties

Properties and compositions	Type of biomass samples	
	OPT	RWS
Proximate analysis		
Moisture content (MC)	7.07 ± 0.04	7.13 ± 0.02
Volatile matter (VM)	71.14 ± 0.20	75.98 ± 0.26
Fixed carbon (FC)	15.42 ± 0.22	15.21 ± 0.24
Ash	6.38 ± 0.02	1.68 ± 0.01
Ultimate analysis (wt.%, dry basis)		
Carbon (C)	45.79 ± 0.07	47.55 ± 0.23
Hydrogen (H)	6.15 ± 0.02	6.22 ± 0.02
Nitrogen (N)	1.47 ± 0.01	0.32 ± 0.01
Oxygen (O)*	46.33 ± 0.07	45.91 ± 0.26
Sulfur (S)	1.47 ± 0.01	0.03 ± 0.01
Lignocellulosic content (wt.%, dry basis)		
Cellulose	46.81 ± 0.36	56.91 ± 0.47
Hemicellulose	23.19 ± 0.14	15.21 ± 0.28
Lignin	9.52 ± 0.09	17.44 ± 0.16
Extractives	20.48 ± 0.16	10.44 ± 0.44
Elemental composition (mg/kg)		
Silicon (Si)	3749	2538
Iron (Fe)	1489	188.6
Calcium (Ca)	5148	5164
Magnesium (Mg)	2647	1058
Sodium (Na)	1126	67.5
Potassium (K)	9749	5037
Higher heating values and lower heating values (MJ/kg)		
HHV	23.02 ± 0.21	23.77 ± 0.19
LHV	21.88 ± 0.18	22.42 ± 0.47
Other properties		
Molecular formula	$CH_{1.597}O_{0.759}$	$CH_{1.556}O_{0.725}$
H/C ratio	1.59	1.55
O/C ratio	0.69	0.67
Bulk density (kg/m³)	150.97 ± 0.36	293.58 ± 0.29

*Calculated by difference method

for pyrolysis applications, influencing heat transfer behavior during pyrolysis. Biomass particle bulk density also refers to energy density (MJ/m³), storage space, handling, and transport costs (McKendry 2002a; Brar et al. 2012; Widjaya et al. 2018).

Thermal analysis

Thermal analysis for OPT and RWS was conducted using a TGA analyzer. Biomass underwent three degradation stages: evaporation of moisture, active pyrolytic stage or volatile release, and passive pyrolytic stage or carbonization. Evaporation of moisture from room temperature to 150 °C took place for all the residues. Mass difference was less than 3% between 150 and 200 °C and was related to extractives

evaporation. Maximum mass loss of volatile release in thermal decomposition occurred between 250 and 450 °C. Thermal results indicated that 6.36% and 4.65% decomposition occurred in the first phase, 64.10% and 68.53% occurred in the second phase, and 2.91% and 3.63% occurred in the third phase, respectively, for OPT and RWS. RWS shows less thermal decomposition in the first stage and more sequentially in the second and third phases. Lesser thermal decomposition is due to less moisture content in woody biomass than non-woody biomass, which decomposes in the first stage. In contrast, high hemicellulose and cellulose contents in RWS result in more degradation in the later two stages. Mean reactivity of RWS is higher than OPT in all the three phases of thermal decomposition as RWS possesses more decomposition than OPT.

The TG and DTG curves migrated towards high-temperature areas as heating rate increased, and thermal hysteresis occurred in the pyrolysis process. Also, when heating rate is elevated, the initial release temperature of volatile components and peak temperatures of DTG curves increase. With the same pyrolysis temperature and heating rate, less volatile matter precipitation, lesser weight loss, and more residual weight were found. The heating rate for slow and flash pyrolysis follows the same trend as normal pyrolysis process. This is because of the decomposition of biomass in the different temperature ranges. Because of higher heating rates, the time duration of vapors released in pyrolytic stage is less in flash pyrolysis than in slow pyrolysis.

Effect of heating rates

Figure 1 represents TG and DTG experiments for OPT and RWS at dynamic heating rates (10 °C/min, 20 °C/min, and 30 °C/min) in an inert gas atmosphere under non-isothermal conditions. It was confirmed from Fig. 1 that increasing rates highly influence thermal decomposition profile. The TGA curve shift occurred in cross-section of biomass due to the development of thermal lag (temperature gradient) because biomass is a weak heat conductor. The temperature profile for cross-section of biomass was presumed to be linear for surface at low temperatures. Biomass' inner core reached same temperature at a particular instance, as adequate heating time was allowed.

Furthermore, temperature profile varied markedly from inner core to outer core along biomass cross-section at a higher heating rate. This was possibly due to a short residence time, which did not provide enough time for two particles to interact. Therefore, the evolution of volatile vapors decreased at a higher heating rate (Maiti et al. 2007).

Figure 1a describes thermal decomposition curves for OPT in argon atmosphere in which average volatilized mass was $73.37 \pm 1.73\%$, accounting for a maximum of 75.57% and

Fig. 1 TG and DTG curves of thermal decomposition of **a**, **c** OPT and **b**, **d** RWS in an atmosphere of nitrogen at different heating rates
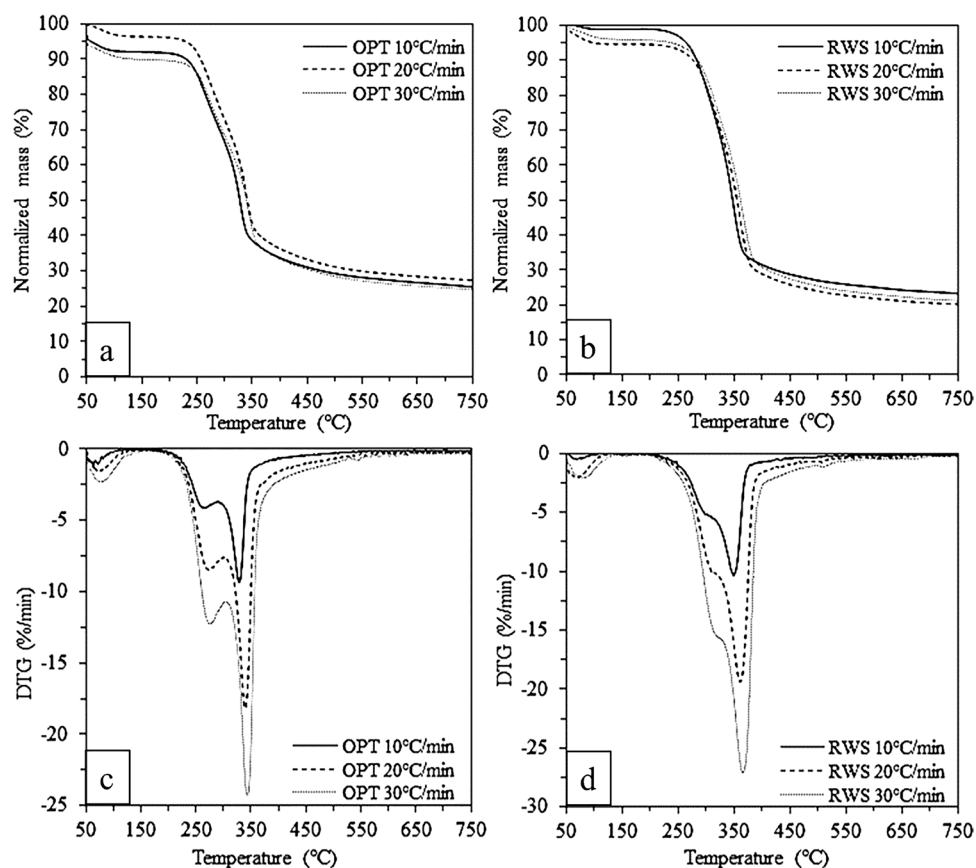
a minimum of 71.34%, at heating rates of 30 and 10 ℃/min, respectively, and corresponding to a 3.5% deviation from average. The volatilization of OPT is associated with two major peaks in the DTG curve shown in Fig. 1b. Depending on heating rate, first peak occurred at 235.4, 244.1, and 244.4 °C and was related to hemicellulose decomposition. In contrast, second peak was found at 317.2, 329.7, and 332.7 °C and related to cellulose decomposition. As shown in Fig. 1c, the mean volatilized mass for RWS was 76.80 ± 2.16%, correlated with one major peak in the DTG curve. Figure 1d presents DTG curves of RWS defined by a single peak due to hemicellulose and cellulose thermal decomposition at 266.6, 276.4, and 280.9 °C for various heating speeds.

Based on the findings, it was also noted that volatile products also increased with a rise in heating rates. However, total residence time increased at lower heating rates, leading to secondary reactions such as re-polymerization and re-condensation that eventually lead to char formation (Maiti et al. 2007). The carbonization step refers to the process of thermal decomposition that occurred in the 450–700 °C temperature range and was only related to remaining biomass thermal decomposition (lignin-based structure). The kinetic degradation response is quite complex for biomass that acquired resistance at lower heating rates and maybe decreased resistance at higher heating rates due to higher

heat and mass transfer across materials favoring a more advanced conversion. It is worth noting that the hypothesis above is true for given biomass, size, and operating conditions (Maiti et al. 2007; Mishra et al. 2019).

Kinetic analysis

Model-free methods (Friedman, OFW, and KAS model) were used to determine kinetic parameters such as activation energy, pre-exponential factor, and reaction order. The biomass kinetic parameters of the Friedman, OFW, and KAS models were calculated using Eqs. (11), (12), and (13). Because of low correlation value, the conversion value greater than 0.7 during model data fitting did not match (Damartzis et al. 2011). The activation energy average values calculated in Friedman, OFW, and KAS model are 259.88 kJ/mol, 266.59 kJ/mol, and 266.50 kJ/mol, respectively, for OPT; and 215.85 kJ/mol, 222.40 kJ/mol, and 222.30 kJ/mol for RWS. For each model, correlation coefficient was above 0.9, which means that experimental data are better suited to this value (Table 2). Activation energy hardly varies with the conversion rate (Table 2), suggesting a higher likelihood of a single-phase reaction occurring (Vyazovkin 2001). The reaction order for the current study is of first order and activation energy can be linearly plot on all the isoconversion plots.

Table 2 Kinetic parameters obtained from model-free methods for OPT and RWS

Conversion	Models								
	Friedman			KAS			OFW		
	E_a (kJ/mol)	R^2	A (min^{-1})	E_a (kJ/mol)	R^2	A (min^{-1})	E_a (kJ/mol)	R^2	R^2
OPT									
0.1	259.58	0.9918	1.36E+02	253.65	0.9918	1.34E+02	253.73	0.9957	1.34E+02
0.2	281.47	0.9939	1.45E+02	267.91	0.9986	1.40E+02	267.98	0.9824	1.40E+02
0.3	303.79	0.9961	1.53E+02	290.79	0.9979	1.50E+02	290.86	0.9762	1.50E+02
0.4	289.96	0.9392	1.42E+02	298.96	0.9705	1.51E+02	299.04	0.9963	1.51E+02
0.5	241.68	0.9801	1.14E+02	272.14	0.9988	1.34E+02	272.22	0.9945	1.34E+02
0.6	218.39	0.9266	1.01E+02	246.29	0.9949	1.18E+02	246.38	0.9949	1.18E+02
0.7	224.36	0.9849	1.04E+02	235.8	0.9819	1.12E+02	235.89	0.9917	1.12E+02
RWS									
0.1	220.33	0.9979	1.78E+01	237.86	0.9818	1.97E+01	237.94	0.9921	1.93E+01
0.2	221.92	0.9705	1.75E+01	222.93	0.9921	1.80E+01	223.03	0.9392	1.79E+01
0.3	228.12	0.9988	1.77E+01	225.12	0.9998	1.79E+01	225.22	0.9392	1.78E+01
0.4	219.84	0.9949	1.67E+01	224.59	0.9928	1.75E+01	224.69	0.9957	1.74E+01
0.5	212.74	0.9824	1.59E+01	219.91	0.9963	1.69E+01	220.02	0.9824	1.68E+01
0.6	208.29	0.9762	1.54E+01	215.13	0.9945	1.63E+01	215.24	0.9762	1.62E+01
0.7	199.73	0.9978	1.47E+01	210.57	0.9849	1.58E+01	210.69	0.9705	1.57E+01
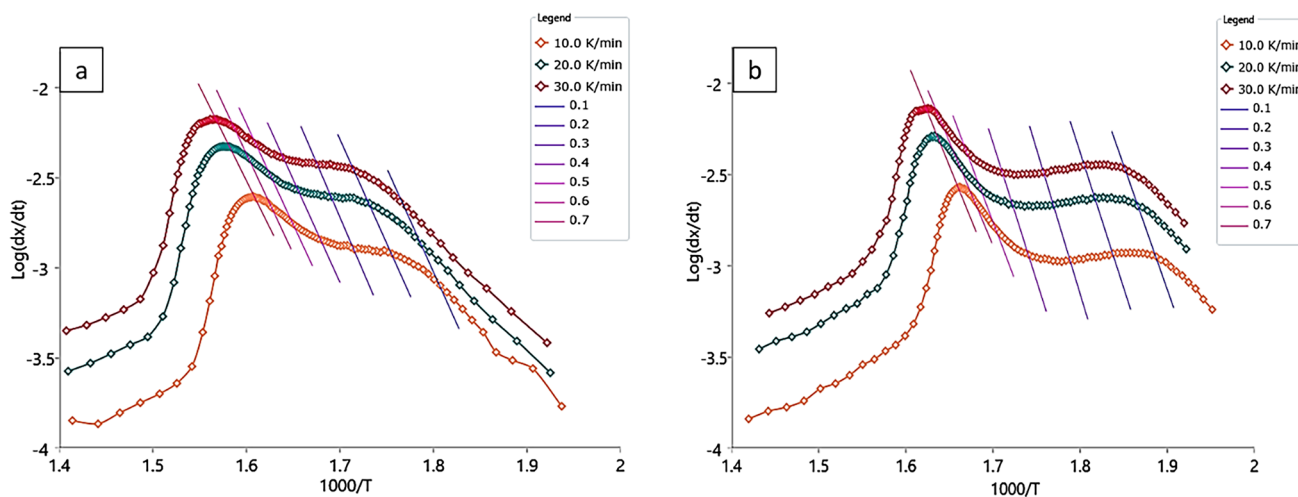
Fig. 2 Friedman method **a** OPT and **b** RWS

The measured activation energy from Friedman method was significantly lower than two other methods. It is an effective method for calculating E_a as it relates to simple differential form of kinetic rate law and does not require an oversimplified approximation since it relates to a differential method that only applies to integral data (TGA) (Heydari et al. 2015; Ojha et al. 2021a). Conversion curves and temperature generate raucous rate data, resulting in very scattered activation energy ranges as shown in Figs. 2, 3, and 4 for Friedman, OFW, and KAS for Figs. 2a, 3a, and 4a as OPT and Figs. 2b,

3b, and 4b as RWS, respectively. One potential explanation for this phenomenon could be that reaction mechanism is not the same as expected.

The correlation coefficient becomes lower when the conversion value exceeds 0.7 and is unsuitable for model fitting. E_a values vary from Friedman, OFW, and KAS models are 218.3 to 303.79 kJ/mol, 235.89 to 299.04 kJ/mol, and 235.8 to 298.96 kJ/mol, respectively, for OPT; and 199.73 to 228.11 kJ/mol, 210.68 to 237.94 kJ/mol, 210.57 to 237.86 kJ/mol, respectively, for RWS with conversion
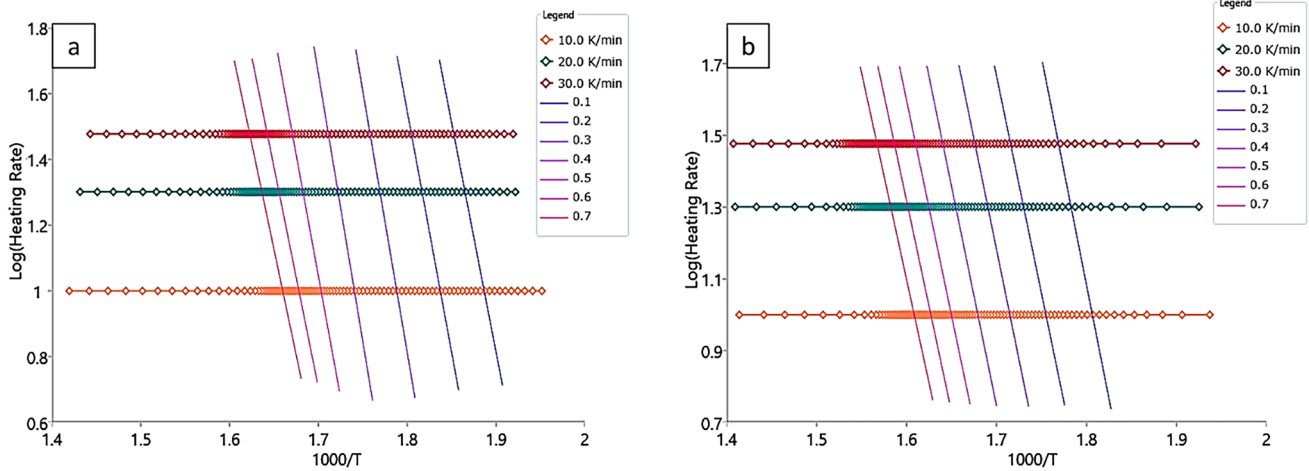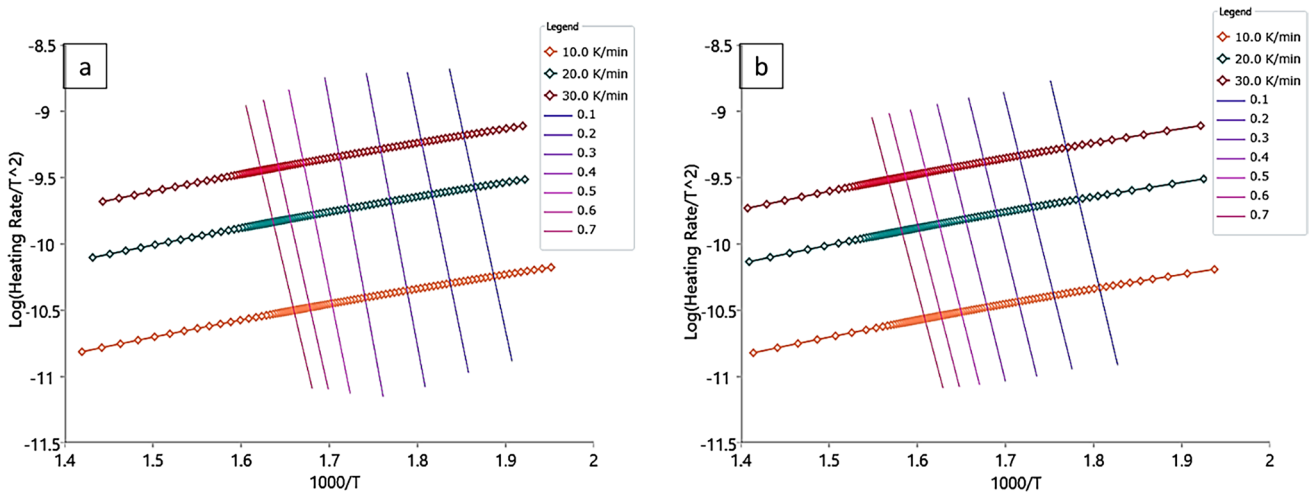
Fig. 3 OFW method **a** OPT and **b** RWS

Fig. 4 KAS method **a** OPT and **b** RWS

value of 0.1 to 0.7. E_a is dependent on pyrolysis reaction mechanism. The activation energy related to the pyrolysis process is directly influenced by the variation in the reaction mechanism. The energy needed to break the specific chemical bonds involved in each phase of the reaction mechanism is represented by the activation energy value for that step. The total activation energy for the pyrolysis reaction is calculated as the sum of these activation energy values (Qiao et al. 2020; Alqarni et al. 2022; De Ras et al. 2022). A higher value of E_a indicates a slower reaction. Gai et al. (2013) reported that E_a could calculate fuel reactivity. In pyrolysis and gasification, fuel reactivity plays an important role (Gai et al. 2013). The thermal breakdown of biomass consists of several processes that may occur simultaneously or independently; therefore, several complex reactions are tightly controlled. However, using a single-step reaction to

characterize the overall process in certain applications, such as reactor modeling and design, is frequent, even if it represents a difficult approximation.

Pyrolysis is a continuous process that implies volatilization increases with an increase in temperature through heat transfer between biomass particles. Conversion is a function of temperature, meaning conversion values increase with an increase in temperature. It decreases after reaching maximum point (0.0023 min^{-1}). A comparable pattern between temperatures and DTG curve has been observed. The apparent activation energy measured is similar to other studies published. In other recorded studies, there was a slight difference in activation energy due to different biomass compositions. Other potential explanations may be various mathematical equations and experimental conditions. The estimated activation energy

Table 3 Py-GC–MS analysis of OPT and RWS biomass (peak area %)

Compounds	Peak area (%)	
	OPT	RWS
2-Propanone	19.55	15.25
Phenol	13.3	11.35
Acetic acid	9.28	13.68
2-Propanone, 1-hydroxy-	4.28	1.65
D-Glucopyranose, 1,6-anhydro-	3.38	-
Acetophenone, 3′,4′-dimethoxy-	3.19	1.67
(E)-2,6-Dimethoxy-4-(prop-1-en-1-yl) phenol	2.89	0.68
Phenol, 2,6-dimethoxy-	2.74	4.18
Toluene	2.13	1.53
Pyridine	2.06	-
2,3-Butanedione	-	1.65
Trans-isoeugenol	1.61	-
Phenol, 2-methoxy-	1.46	3.14
2,3-Anhydro-d-mannosan	1.45	1.27
1,2-Cyclopentanedione	-	1.33
2-Methoxy-4-vinylphenol	1.28	-
2-Methoxy-4-methyl-phenol	-	1.26

increased up to 50% by an increase in convertible value. Decomposition of individual biomass components such as cellulose, hemicellulose, lignin, extractive components, and other mineral components decreased. Another plausible explanation may be adopting various approximations (Mishra and Mohanty 2020). In addition, models' activation energy shifts due to approximations taken.

Gas chromatography using pyrolyzer

OPT and RWS biomass underwent Py-GC–MS analysis and obtained mass spectra matched with NIST library. Specific values of peak area percentage for each compound were listed in Table 3. Pyrolysis of biomass mainly produces phenols, esters, ethers, aromatics, furans, high-carbon alkanes, ketones, etc., making it more attractive to convert biomass into biomass biofuels (Chen et al. 2015; Mishra and Mohanty 2020). Also, aromatic hydrocarbons, cycloalkane, furanic compounds, acids, kenotic compounds, and miscellaneous hydrocarbon can be obtained from thermochemical conversion of biomass containing hemicellulose and cellulose (Liaw et al. 2014; Du et al. 2023).

Furthermore, the current study confirms the presence of aromatics, hydrocarbons, ester, ethers, ketones, etc., as given in Table 3. Carbonyl compounds such as ketones and aldehydes can be produced by reducing carboxylic acids. It will also result in the further conversion of various alcohols to various hydrocarbons. At higher temperatures, decarboxylation of carboxylic acids can promote lower amounts of acids (Anand et al. 2017; Gautam and Vinu 2018). Water molecules form during pyrolysis when oxygen molecules from biomass react with hydrogen.

Moreover, it reduces reaction and forms carbon dioxide at higher temperature. Phenols formed in the pyrolysis of OPT are generally higher than RWS. In contrast, acetic acid formed in RWS is higher than OPT because of decarbonylation and decarboxylation of woody and non-woody biomass, respectively. This could also be attributed to producing CO by reducing CO_2 over char. At 550 °C, stable structural biomass fragmented into lower molecular weight compounds, which cannot be achieved at a lower temperature (Yang et al. 2014; Ma et al. 2022). RWS shows higher presence of desired products (hydrocarbons, alcohols, etc.) indebted to enhanced cracking of volatile fraction into non-condensable gases than OPT. Furthermore, deamination results in formation of nitrogenous compounds decreased, as shown in Py-GC–MS results.

Conclusions

Thermogravimetric research examined pyrolysis behavior and thermal stability of oil palm trunk (OPT) and rubberwood sawdust biomass (RWS). TG thermograph reported that without damaging decomposition behavior, degradation peak moved to higher region with increased heating rate. OPT in argon atmosphere in which average volatilized mass was $73.37 \pm 1.73\%$, accounting for a maximum of 75.57% and a minimum of 71.34%, at heating rates of 30 and 10 °C/min, respectively. The mean volatilized mass for RWS was $76.80 \pm 2.16\%$, correlated with one major peak in the DTG curve. Also, RWS shows 4.37 min higher to reach maximum rate of evolution than OPT because of its woody nature. The activation energy varied from 218.4 to 303.8 kJ/mol (Friedman), 235.9 to 299.1 kJ/mol (OFW), and 235.8 to 298.9 kJ/mol (KAS) for OPT; and 199.7 to 228.1 kJ/mol (Friedman), 210.6 to 225.6 kJ/mol (OFW), and 210.7 to 225.2 kJ/mol (KAS) for RWS. Both biomasses verified their bioenergy ability through physiochemical characterization of lower activation energy and high cellulosic contents. In raw biomass, FTIR analysis verified existence of useful functional groups. RWS resulted in 19.64% peak area corresponding to phenol derivatives, while OPT yielded nearly 17.87% peak area corresponding to linear organics. This study's kinetic analysis and Py-GC–MS data can be used for reactor design, optimization, and development. Lignocellulosic biomass with high hemicellulose and cellulose contents can be used as feedstocks for electricity generation.

Declarations

Ethics approval Not applicable.

Consent to participate Not applicable.

Consent for publication Not applicable.

Competing interests The authors declare no competing interests.

References

Alqarni AO, Nabi RAU, Althobiani F, et al (2022) Statistical optimization of pyrolysis process for thermal destruction of plastic waste based on temperature-dependent activation energies and pre-exponential factors. Processes 10. https://doi.org/10.3390/pr10081559

Alwani MS, Abdul Khalil HPS, Sulaiman O et al (2014) An approach to using agricultural waste fibres in biocomposites application: thermogravimetric analysis and activation energy study. BioResources 9:218–230. https://doi.org/10.15376/biores.9.1.218-230

Anand V, Gautam R, Vinu R (2017) Non-catalytic and catalytic fast pyrolysis of Schizochytrium limacinum microalga. Fuel 205:1–10. https://doi.org/10.1016/j.fuel.2017.05.049

Biswas B, Pandey N, Bisht Y et al (2017) Pyrolysis of agricultural biomass residues: comparative study of corn cob, wheat straw, rice straw and rice husk. Bioresour Technol 237:57–63. https://doi.org/10.1016/j.biortech.2017.02.046

Brar JS, Singh K, Wang J, Kumar S (2012) Cogasification of coal and biomass: a review. Int J for Res 2012:1–10. https://doi.org/10.1155/2012/363058

Ceylan S, Topçu Y (2014) Pyrolysis kinetics of hazelnut husk using thermogravimetric analysis. Bioresour Technol 156:182–188. https://doi.org/10.1016/j.biortech.2014.01.040

Chen B, Zhou D, Zhu L (2008) Transitional adsorption and partition of nonpolar and polar aromatic contaminants by biochars of pine needles with different pyrolytic temperatures. Environ Sci Technol 42:5137–5143. https://doi.org/10.1021/es8002684

Chen L, Wang X, Yang H et al (2015) Study on pyrolysis behaviors of non-woody lignins with TG-FTIR and Py-GC/MS. J Anal Appl Pyrolysis 113:499–507. https://doi.org/10.1016/j.jaap.2015.03.018

Damartzis T, Vamvuka D, Sfakiotakis S, Zabaniotou A (2011) Thermal degradation studies and kinetic modeling of cardoon (Cynara cardunculus) pyrolysis using thermogravimetric analysis (TGA). Bioresour Technol 102:6230–6238. https://doi.org/10.1016/j.biortech.2011.02.060

Du J, Dou B, Zhang H et al (2023) Non-isothermal kinetics of biomass waste pyrolysis by TG-MS/DSC. Carbon Capture Sci Technol 6:100097. https://doi.org/10.1016/j.ccst.2023.100097

Gai C, Dong Y, Zhang T (2013) The kinetic analysis of the pyrolysis of agricultural residue under non-isothermal conditions. Bioresour Technol 127:298–305. https://doi.org/10.1016/j.biortech.2012.09.089

Gautam R, Vinu R (2018) Non-catalytic fast pyrolysis and catalytic fast pyrolysis of Nannochloropsis oculata using Co-Mo/γ-Al2O3 catalyst for valuable chemicals. Algal Res 34:12–24. https://doi.org/10.1016/j.algal.2018.06.024

Heydari M, Rahman M, Gupta R (2015) Kinetic study and thermal decomposition behavior of lignite coal. Int J Chem Eng 2015:1–9. https://doi.org/10.1155/2015/481739

Hu X, Gholizadeh M (2019) Biomass pyrolysis: a review of the process development and challenges from initial researches up to the commercialisation stage. J Energy Chem 39:109–143. https://doi.org/10.1016/j.jechem.2019.01.024

Huang X, Cao J-P, Zhao X-Y et al (2016) Pyrolysis kinetics of soybean straw using thermogravimetric analysis. Fuel 169:93–98. https://doi.org/10.1016/j.fuel.2015.12.011

Li J, Dou B, Zhang H et al (2021) Pyrolysis characteristics and non-isothermal kinetics of waste wood biomass. Energy 226:120358. https://doi.org/10.1016/j.energy.2021.120358

Liaw S-S, Haber Perez V, Zhou S et al (2014) Py-GC/MS studies and principal component analysis to evaluate the impact of feedstock and temperature on the distribution of products during fast pyrolysis. J Anal Appl Pyrolysis 109:140–151. https://doi.org/10.1016/j.jaap.2014.06.018

Loh SK (2017) The potential of the Malaysian oil palm biomass as a renewable energy source. Energy Convers Manag 141:285–298

Ma M, Xu D, Zhi Y et al (2022) Co-pyrolysis re-use of sludge and biomass waste: development, kinetics, synergistic mechanism and industrialization. J Anal Appl Pyrolysis 168:105746. https://doi.org/10.1016/j.jaap.2022.105746

Maiti S, Purakayastha S, Ghosh B (2007) Thermal characterization of mustard straw and stalk in nitrogen at different heating rates. Fuel 86:1513–1518. https://doi.org/10.1016/j.fuel.2006.11.016

McKendry P (2002a) Energy production from biomass (part 1): overview of biomass. Bioresour Technol 83:37–46. https://doi.org/10.1016/S0960-8524(01)00118-3

Mckendry P (2002b) Energy production from biomass (part 2): conversion technologies. Bioresour Technol 83:47–54. https://doi.org/10.1016/S0960-8524(01)00119-5

Mishra RK, Mohanty K (2018) Pyrolysis kinetics and thermal behavior of waste sawdust biomass using thermogravimetric analysis. Bioresour Technol 251:63–74. https://doi.org/10.1016/j.biortech.2017.12.029

Mishra RK, Mohanty K (2019) Pyrolysis characteristics, fuel properties, and compositional study of Madhuca longifolia seeds over metal oxide catalysts. Biomass Convers Biorefin. https://doi.org/10.1007/s13399-019-00469-3

Mishra RK, Mohanty K (2020) Pyrolysis characteristics, fuel properties, and compositional study of Madhuca longifolia seeds over metal oxide catalysts. Biomass Convers Biorefin 10:621–637. https://doi.org/10.1007/s13399-019-00469-3

Mishra RK, Sahoo A, Mohanty K (2019) Pyrolysis kinetics and synergistic effect in co-pyrolysis of Samanea saman seeds and polyethylene terephthalate using thermogravimetric analyser. Bioresour Technol 289:121608. https://doi.org/10.1016/j.biortech.2019.121608

Mishra RK, Kumar V, Mohanty K (2020) Pyrolysis kinetics behaviour and thermal pyrolysis of Samanea saman seeds towards the production of renewable fuel. J Energy Inst 93:1148–1162. https://doi.org/10.1016/j.joei.2019.10.008

Mishra A, Nanda S, RanjanParida M et al (2023) A comparative study on pyrolysis kinetics and thermodynamic parameters of little millet and sunflower stems biomass using thermogravimetric analysis. Bioresour Technol 367:128231. https://doi.org/10.1016/j.biortech.2022.128231

Mohan D, Pittman CU, Steele PH (2006) Pyrolysis of wood/biomass for bio-oil: a critical review. Energy Fuels 20:848–889. https://doi.org/10.1021/ef0502397

Ojha DK, Viju D, Vinu R (2021) Fast pyrolysis kinetics of lignocellulosic biomass of varying compositions. Energy Convers Manag X 10:100071. https://doi.org/10.1016/J.ECMX.2020.100071

Palamanit A, Khongphakdi P, Tirawanichakul Y, Phusunti N (2019) Investigation of yields and qualities of pyrolysis products obtained from oil palm biomass using an agitated bed pyrolysis reactor. Biofuel Res J 6:1065–1079. https://doi.org/10.18331/BRJ2019.6.4.3

Pattanayak S, Hauchhum L, Loha C et al (2021) Experimental investigation on pyrolysis kinetics, reaction mechanisms and thermodynamic parameters of biomass and tar in N2 atmosphere. Sustain Energy Technol Assess 48:101632. https://doi.org/10.1016/j.seta.2021.101632

Pattiya A, Suttibak S (2012a) Production of bio-oil via fast pyrolysis of agricultural residues from cassava plantations in a fluidised-bed reactor with a hot vapour filtration unit. J Anal Appl Pyrolysis 95:227–235. https://doi.org/10.1016/j.jaap.2012.02.010

Pattiya A, Suttibak S (2012b) Influence of a glass wool hot vapour filter on yields and properties of bio-oil derived from rapid pyrolysis of paddy residues. Bioresour Technol 116:107–113. https://doi.org/10.1016/j.biortech.2012.03.116

Peterson CA, Hornbuckle MK, Brown RC (2022) Biomass pyrolysis devolatilization kinetics of herbaceous and woody feedstocks. Fuel Process Technol 226:107068. https://doi.org/10.1016/j.fuproc.2021.107068

Pielsticker S, Gövert B, Umeki K, Kneer R (2021) Flash pyrolysis kinetics of extracted lignocellulosic biomass components. Front. Energy Res 9:737011. https://doi.org/10.3389/fenrg.2021.737011

Qiao Y, Das O, Zhao SN et al (2020) Pyrolysis kinetic study and reaction mechanism of epoxy glass fiber reinforced plastic by thermogravimetric analyzer (Tg) and tg–ftir (fourier-transform infrared) techniques. Polymers (basel) 12:1–16. https://doi.org/10.3390/polym12112739

De Ras K, Kusenberg M, Vanhove G, et al (2022) A detailed experimental and kinetic modeling study on pyrolysis and oxidation of oxymethylene ether-2 (OME-2). Combust Flame 238. https://doi.org/10.1016/j.combustflame.2021.111914

Rueda-Ordóñez YJ, Arias-Hernández CJ, Manrique-Pinto JF et al (2019) Assessment of the thermal decomposition kinetics of empty fruit bunch, kernel shell and their blend. Bioresour Technol 292:121923. https://doi.org/10.1016/j.biortech.2019.121923

Shahbandeh M (2020) Production volume of palm oil worldwide from 2012/13 to 2019/20. In: Statista. https://www-statista-com.ezproxy.cardiffmet.ac.uk/statistics/613466/olive-oil-production-volume-worldwide/. Accessed 21 Mar 2022

Shrivastava P, Khongphakdi P, Palamanit A et al (2020) Investigation of physicochemical properties of oil palm biomass for evaluating potential of biofuels production via pyrolysis processes. Biomass Convers Biorefin. https://doi.org/10.1007/s13399-019-00596-x

Shuit SH, Tan KT, Lee KT, Kamaruddin AH (2009) Oil palm biomass as a sustainable energy source: a Malaysian case study. Energy 34:1225–1235. https://doi.org/10.1016/j.energy.2009.05.008

Slopiecka K, Bartocci P, Fantozzi F (2012) Thermogravimetric analysis and kinetic study of poplar wood pyrolysis. Appl Energy 97:491–497. https://doi.org/10.1016/j.apenergy.2011.12.056

Sulaiman F, Abdullah N, Gerhauser H, Shariff A (2011) An outlook of Malaysian energy, oil palm industry and its utilization of wastes as useful resources. Biomass Bioenerg. https://doi.org/10.1016/j.biombioe.2011.06.018

Tian B, Wang X, Zhao W et al (2021) Pyrolysis behaviors, kinetics and gaseous product evolutions of two typical biomass wastes. Catal Today 374:77–85. https://doi.org/10.1016/j.cattod.2020.12.023

Uzun BB, Varol EA, Pütün E (2016) Pyrolysis: a sustainable way from biomass to biofuels and biochar. In: Bruckman VJ, Apaydin Varol E, Uzun BB, Liu J (eds) Biochar. Cambridge University Press, Cambridge, pp 239–265

Vyazovkin S (2001) Modification of the integral isoconversional method to account for variation in the activation energy. J Comput Chem 22:178–183. https://doi.org/10.1002/1096-987X(20010130)22:23.0.CO;2-%23

Widjaya ER, Chen G, Bowtell L, Hills C (2018) Gasification of nonwoody biomass: a literature review. Renew Sustain Energy Rev 89:184–193. https://doi.org/10.1016/j.rser.2018.03.023

Xiao R, Yang W, Cong X et al (2020) Thermogravimetric analysis and reaction kinetics of lignocellulosic biomass pyrolysis. Energy 201:117537. https://doi.org/10.1016/j.energy.2020.117537

Yaman S (2004) Pyrolysis of biomass to produce fuels and chemical feedstocks. Energy Convers Manag 45:651–671. https://doi.org/10.1016/S0196-8904(03)00177-8

Yang X, Zhang R, Fu J et al (2014) Pyrolysis kinetic and product analysis of different microalgal biomass by distributed activation energy model and pyrolysis–gas chromatography–mass spectrometry. Bioresour Technol 163:335–342. https://doi.org/10.1016/j.biortech.2014.04.040

Yusoff S (2006) Renewable energy from palm oil – innovation on effective utilization of waste. J Clean Prod 14:87–93. https://doi.org/10.1016/j.jclepro.2004.07.005